Mon. Not. R. Astron. Soc. **353,** 153–161 (2004) doi:10.1111/j.1365-2966.2004.08058.x

Hydrogen in the atmosphere of the evolved WN3 Wolf–Rayet star WR 3: defying an evolutionary paradigm?

S. V. Marchenko,[1⋆] A. F. J. Moffat,[2⋆] P. A. Crowther,[3⋆] A.-N. Chené,[2⋆] M. De Serres,[4⋆] P. R. J. Eenens,[5,6⋆] G. M. Hill,[7⋆] J. Moran[8⋆] and T. Morel[9⋆]

[1]*Department of Physics and Astronomy, Western Kentucky University, Bowling Green, KY 42101-3576, USA*
[2]*Département de Physique, Université de Montréal, C.P. 6128, Succ. 'Centre-Ville', Montréal, QC, H3C 3J7, Canada, and Observatoire du mont Mégantic*
[3]*Department of Physics and Astronomy, University of Sheffield, Hicks Building, Hounsfield Road, Sheffield S3 7RH*
[4]*Physics Department, McGill University, Rutherford Physics Building, 3600 University St, Montreal, QC, H3A 2T8, Canada*
[5]*Institut d'Astrophysique, Université de Liège, Allée du 6 Août 17 (B5C), B - 4000 Liège (Sart Tilman), Belgium*
[6]*Department of Astronomy, University of Guanajuato, 36000 Guanajuato, GTO, Mexico*
[7]*W.M. Keck Observatory, 65-1120 Mamalahoa Hwy, Kamuela, HI 96743, USA*
[8]*Department of Physics and Astronomy, University of North Carolina, Phillips Hall, CB #3255, Chapel Hill, NC 27599-3255, USA*
[9]*Istituto Nazionale di Astrofisica, Osservatorio Astronomico di Palermo G.S. Vaiana, Piazza del Parlamento 1, I-90134 Palermo, Italy*

Accepted 2004 May 20. Received 2004 May 19; in original form 2004 April 9

ABSTRACT

WR 3 is the brightest very early-type WN star in the sky. Based on several years of time-resolved spectroscopy and precision photometry on various time-scales, we deduce that WR 3 is most likely a single, weak-lined star of type WN3ha (contrary to its current catalogue-type of WN3 + O4), with H lines occurring both in emission and absorption in its wind. This conclusion is confirmed and strengthened via detailed modelling of the spectrum of WR 3. Given the similarity of WR 3 with numerous H-rich WNE stars in the Large Magellanic Cloud and especially the Small Magellanic Cloud, and its location towards the metal-deficient exterior of the Galaxy, we conclude that rotationally induced meridional circulation probably led to the apparently unusual formation of this hot Galactic WN star with enhanced hydrogen. Although we cannot completely rule out the possibility of a binary with a low orbital inclination and/or long period, we regard this latter possibility as highly unlikely.

Key words: stars: abundances – stars: individual: WR 3 – stars: Wolf–Rayet.

1 INTRODUCTION

WR 3 (HD 9974) is the brightest very early-type WN star in the sky. In the VIIth Catalogue of Galactic Wolf–Rayet stars (van der Hucht 2001) WR 3 is classified as WN3+O4, i.e. as an early-type nitrogen-sequence WR star with an O-type companion. Its binary nature was supported by three pieces of evidence, as follows.

(i) It was noted by many authors (e.g. Nugis & Niedzielski 1995; Smith, Shara & Moffat 1996; Smith & Maeder 1998; van der Hucht 2001) that the emission lines seem to be too weak in WR 3 compared to other presumably single WR stars of similar spectral class, which may be related to dilution by the continuum flux of a close companion.

⋆E-mail: sergey@astro.wku.edu (SVM); moffat@astro.umontreal.ca (AFJM); Paul.Crowther@sheffield.ac.uk (PAC); chene@astro.umontreal.ca (ANC); deserres@astro.umontreal.ca (MD); eenens@astro.ulg.ac.be (PRJE); ghill@keck.hawaii.edu (GMH); moranj@physics.unc.edu (JM); morel@oapa.astropa.unipa.it (TM)

(ii) Blended with the broad WR emissions, there are well-defined absorption lines mimicking an early-type O-star spectrum.

(iii) Both the absorption and the emission lines were claimed to move in phase with a low-amplitude, tentative period $P = 46\overset{\mathrm{d}}{.}85 \pm 0\overset{\mathrm{d}}{.}02$, $K(\mathrm{WR}) = 33$ km s^{-1} (Moffat et al. 1986). Combined with the high displacement from the Galactic plane – $z = -429$ pc (van der Hucht 2001), although probably not so strange, given its position in the Galaxy and the warp of the Galactic plane – this was taken to signify that WR 3 is a runaway system that harbours a compact companion, presumably a neutron star.

The binary nature of WR 3 was already questioned by Massey & Conti (1981). They found no apparent long-term (dozens of years) changes in the radial velocities (RVs) and placed a $K \lesssim 25$ km s^{-1} limit on the semi-amplitude of any orbital motion for periods $P \lesssim 2$ yr. Obviously, this did not eliminate a very wide binary, either physical or optical. The apparent weakness of emission features prompted Hamann & Koesterke (1998) to ascribe WR 3 to the weak-lined category of single WNE stars (see also Smith & Maeder 1998).

Assuming single status for WR 3, one must accept the presence of a sizable amount of hydrogen in the WN atmosphere. This leads

Table 1. New RV measurements of the emission and absorption components in the WR 3 spectrum. The full table is available from http://www.blackwellpublishing.com/products/journals/suppmat/MNR/MNR8058/MNR8058sm.htm.

HJD 2440000	Observatory	RV(em) km s^{-1}	σ(em) km s^{-1}	RV(abs) km s^{-1}	σ(abs) km s^{-1}	HJD 2440000	Observatory	RV(em) km s^{-1}	σ(em) km s^{-1}	RV(abs) km s^{-1}	σ(abs) km s^{-1}
8284.642	OMM	−10.5	7.9	−44.6	15.2	9265.938	SPM	−12.7	9.9	−11.6	16.7
8287.654	OMM	21.6	19.0	41.2	16.0	9267.898	SPM	−0.8	12.4	−3.5	9.9
8289.672	OMM	24.5	19.2	68.2	9.8	9637.812	OMM	6.3	6.5	20.4	18.9
8762.782	OMM	−4.0	0.6	−52.5	35.4	9638.826	OMM	−0.6	7.2	21.5	8.8
8802.817	OMM	16.3	4.2	−33.8	49.4	9640.821	OMM	−7.3	6.6	27.8	8.8

to a paradox: the standard evolutionary tracks of WR stars predicted a practical absence of hydrogen in an evolved, single, hot WN3 star. However, WR 3 may not be unique. Hydrogen is clearly present in the presumably single, early-type galactic stars WR 128 (WN4) and WR 152 (WN3) (Crowther, Smith & Hillier 1995; Nugis & Niedzielski 1995), as well as in many of the early-type WN stars in the Large Magellanic Cloud (LMC) and especially in the Small Magellanic Cloud (SMC; Foellmi, Moffat & Guerrero 2003a,b; Foellmi 2004), where the cause is believed to be low-Z induced rapid rotation and lower mass loss of the WR progenitor, leading to greater mixing and a prolonged H-rich WN stage (Maeder & Meynet 2001, and references therein). High hydrogen content was also suspected in WR 3 (Conti, Leep & Perry 1983). In an attempt to clarify the question of binarity and to address the problem of the surprisingly high hydrogen content for a Galactic WNE star, we organized a programme of systematic, long-term spectral monitoring interspersed with occasional photometry. Below, we discuss the results of the monitoring and perform a quantitative analysis of the spectrum of WR 3.

2 OBSERVATIONS AND DATA REDUCTION

During a long-term spectroscopic monitoring campaign, we used the facilities at three different sites.

(i) In 1991–2001 we acquired data at the 1.6-m telescope of the Mont Mégantic Observatory (OMM; Québec, Canada) with the attached Cassegrain spectrograph and a variety of CCDs. In 1991–1994 the spectra covered the λλ4400–5000 spectral region with $\Delta\lambda = 2.5$–3.0 Å (three pixel) resolution. The 10–60 min exposures yielded a signal-to-noise (S/N) of 80–350 in the continuum adjacent to the He II 4686-Å line. We also took occasional spectra in different spectral regions, λλ4000–4500 or λλ5000–6600. In 2000–2001 we changed the approach in an attempt to investigate the short-term line profile variability. We acquired higher-resolution spectra ($\Delta\lambda =$ 0.66 Å, three pixel) in the λλ4250–5150 region with shorter exposure times, 10–30 min. For the purposes of this paper we combined the subsequent exposures, producing one to three average spectra per night with S/N = 80–270.

(ii) In 1993 September–October, we used the 2.1-m telescope of the San Pedro Mártir Observatory (SPM; Baja California, Mexico), covering with a 1024 × 1024 Thompson CCD the λλ4000–4900 region with $\Delta\lambda = 2.50$ Å (three pixel) spectral resolution. Each night we took multiple spectra with 10–20 min individual exposure times. During the final processing, the sequences of short-exposure spectra were combined to reach S/N = 110–220.

(iii) In 1996 October–November, the 1.8-m telescope of the Dominion Astrophysical Observatory (DAO; British Columbia, Canada) provided λλ5100–6100 spectral coverage with $\Delta\lambda =$ 1.44 Å (three pixel) resolution. Each night we acquired multiple 30-min exposures, subsequently combining them to reach S/N = 90–130 in the continuum of a nightly-averaged spectrum.

All the CCD spectra were processed with IRAF. Merging the multi-epoch spectral data, we used, if appropriate, the diffuse IS features at 4501 and 4762 Å to co-align the individual spectra. This careful refinement of the original wavelength calibration provided relatively good long-term stability of the measurements, with systematic deviations between different subsets not exceeding 10 km s^{-1}. Finally, we constructed a spectral template and used it for measurements of RVs. This was done in two steps. First of all, we grouped the spectra in accordance with the place (observatory by observatory) and the epoch of observations. Then, by intercomparison of the averages we deduced that by combining them into an overall average template we do not degrade quality. Hence, we produced a weighted mean of the individual groups, taking the numbers of observations as weights. This average spectrum was used as a template in cross-correlation with individual spectra in the 4400–5000 Å region. We applied the same technique to the half-dozen OMM and DAO spectra in the 5300–6000 Å spectral range.

RVs of the absorption components were obtained by:

(i) measuring the centroid-based wavelengths of the prominent absorption dips at 4337 (if available), 4538 and 4855 Å in the template spectrum;
(ii) repeating the measurements in the individual spectra;
(iii) calculating RVs for each absorption dip as a difference between the individual and template RVs;
(iv) yielding the final results by simple averaging of the RVs of the absorptions.

In Table 1 we list the heliocentric Julian dates along with the RVs and their errors for the emission and absorption components. The full table is available from http://www.blackwellpublishing.com/products/journals/suppmat/MNR/MNR8058/MNR8058sm.htm.

In 2003 November, we used the 1.3-m Robotically Controlled Telescope (RCT), located at Kitt Peak (Arizona, USA).[1] We took a series of short-exposure (20–200 s, depending on the filter) *UBV* (Johnson) images (9 × 9 arcmin^2 field), then combined them in an attempt to study the field around WR 3 and to detect a visual companion, if any.

We also observed WR 3 photometrically on two occasions.

(i) On 1993 September 16–October 3 (simultaneously with a spectroscopic run), we used the single-channel photometer attached to the 0.84-m telescope of the SPM and a narrow-band filter ($\lambda_c =$ 7000 Å, FWHM = 175 Å) which sampled a practically line-free region of the stellar continuum. A typical observation consisted of

[1] For more information, see http://rct.kpno.noao.edu.

Table 2. Photometry of WR 3 in 1993. The full table is available from http://www.blackwellpublishing.com/products/journals/suppmat/MNR/MNR8058/MNR8058sm.htm.

HJD 2449200	WR–c1 mag	WR–c2 mag	HJD 2449200	WR–c1 mag	WR–c2 mag	HJD 2449200	WR–c1 mag	WR–c2 mag
47.9501	−1.366	−1.322	53.8700	−1.346	−1.304	58.9181	−1.353	−1.308
47.9694	−1.367	−1.322	53.8901	−1.337	−1.305	58.9344	−1.356	−1.314
47.9867	−1.341	−1.298	53.9063	−1.348	−1.305	58.9521	−1.365	−1.320
48.0020	−1.336	−1.290	53.9228	−1.347	−1.310	58.9704	−1.365	−1.316
48.8746	−1.367	−1.323	53.9394	−1.347	−1.310	58.9869	−1.362	−1.319

Table 3. Photometry of WR 3 in 1996. The full table is available from http://www.blackwellpublishing.com/products/journals/suppmat/MNR/MNR8058/MNR8058sm.htm.

HJD 2450300	WR–c1 mag	WR–c2 mag	WR–c3 mag	HJD 2450300	WR–c1 mag	WR–c2 mag	WR–c3 mag	HJD 2450300	WR–c1 mag	WR–c2 mag	WR–c3 mag
47.924	−1.030	−1.337	−0.962	54.969	−1.044	−1.349	−0.979	59.732	−1.055	−1.372	−0.996
47.944	−1.035	−1.344	−0.956	54.982	−1.036	−1.349	−0.976	59.746	−1.052	−1.372	−0.993
47.967	−1.054	−1.357	−0.984	55.700	−1.026	−1.359	–	59.785	−1.059	−1.380	−1.004
47.983	−1.040	−1.357	−0.978	55.716	−1.048	−1.361	−0.977	59.799	−1.067	−1.379	−1.001
47.998	−1.041	−1.362	−0.977	55.758	−1.052	−1.362	−0.981	59.864	−1.046	−1.368	−0.993

a 120-s integration following the sequence, c2–sky–c1–wr–c1–wr–c1–sky–c2, with GSC 03683−02162 as c1 and HD 236797 as c2. During the data processing, we have averaged all the values within one sequence. This resulted in 129 observations (Table 2; the full table is available from http://www.blackwellpublishing.com/products/journals/suppmat/MNR/MNR8058/MNR8058sm.htm.). Both the comparison stars and the simultaneously observed bright main-sequence stars (HR 7672, HR 7689, HR 7693 and HR 7697) were used to derive an average extinction coefficient, $k(7000\ \text{Å}) = 0.044 \pm 0.021$. Excellent observing conditions helped to achieve very good accuracy, $\sigma(\text{c1–c2}) = 0.003$ mag, while both $\sigma(\text{WR–c1}) = 0.008$ mag and $\sigma(\text{WR–c2}) = 0.009$ mag pointed to the very low, but non-zero, activity of the star, as compared to other Galactic WR stars (Lamontagne & Moffat 1987; Marchenko et al. 1998a,b)

(ii) In 1996 September (see more details in Morel et al. 1999) we repeated observations with the same configuration, the 0.84-m telescope and the single-channel photometer, this time using a different narrow-band filter with $\lambda_c = 5140$ Å and FWHM = 90 Å. This also allowed us to isolate the region dominated by the stellar continuum flux. The chosen comparison stars provided the following mean precisions: $\sigma(\text{c1–c2}) = 0.006$ mag, $\sigma(\text{c1–c3}) = 0.007$ mag, $\sigma(\text{c2–c3}) = 0.007$ mag for 115 observations (Table 3; the full table is available from http://www.blackwellpublishing.com/products/journals/suppmat/MNR/MNR8058/MNR8058sm.htm.), and $\sigma(\text{WR–c1}) = \sigma(\text{WR–c2}) = \sigma(\text{WR–c3}) = 0.010$ mag. We added to c1 and c2 one more comparison star, c3 (GSC 03683−01926).

3 PERIOD SEARCH

In order to look for signs of orbital motion, we used two approaches. In search of long-term variations we combined the RV data from Table 1 (where each point represents the nightly-averaged data) with measurements from Massey & Conti (1981) and Moffat et al. (1986). Treating the RVs of absorption and emission lines separately, we applied the period search routine based on the algorithm of Roberts, Lehár & Dreher (1987). In both samples, we found no periodic signals with false-alarm probability (e.g. Scargle 1982) below 0.1. This places the following limits on the RV variations for a binary with eccentricity $0 \leqslant e \lesssim 0.5$ in the range of orbital periods between 2 d and 23 yr: for the emission component (100 measurements), the amplitude of a hypothetical sinusoidal signal cannot exceed $K = 8$ km s^{-1}; for the absorption component (86 measurements) $K < 20$ km s^{-1}.

In an attempt to reveal any short-term, periodic RV variations, we analysed all the data secured during the intense spectral monitoring in 1993 (SPM), 1994 (OMM) and 2001 (OMM). Typically, each night of observation provided up to three spectra. Would the absorption and emission details move in antiphase, this would be readily detected. This is apparently not the case for WR 3, where a plot of RV_{abs} versus RV_{em} produces a scatter diagram which is slightly elongated along the y-axis (Fig. 1). We relate this elongation to the difference in the measurement errors for the emission and absorption components. The correlation coefficient, $r = -0.16$ (for

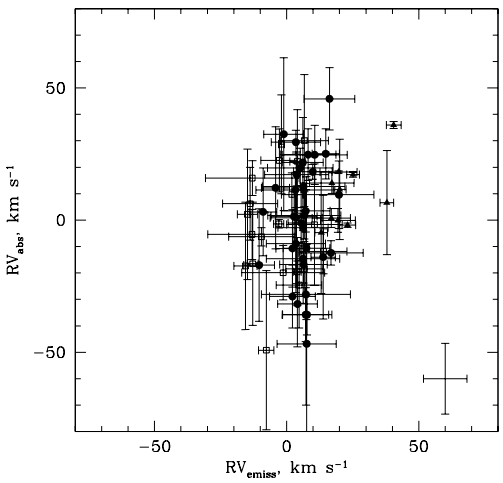

Figure 1. Short-term variability of the RVs of the emission and absorption components. Open squares denote the 1993 data from SPM; filled circles mark the 1994 OMM data and filled triangles show the 2001 OMM measurements. In the lower-right corner we plot the representative 2σ error bars.

65 observations), is too low to consider the short-term variations as interdependent.

Based on the results of our 1993 and 1996 photometry, WR 3 should be considered as variable. However, the star's activity remains at a very low level and seems to be random. In both data sets we find no periodic signals exceeding the corresponding 95 per cent confidence levels, i.e. the peak-to-valley amplitude of any hypothetical periodic signal cannot exceed ∼0.01 mag.

4 WR 3: SINGLE STAR OR BINARY?

With a wealth of new data, we try to answer the question: is WR 3 a binary or a single star? Considering the invariably negative results of the searches for signs of periodic variability in the stellar flux and RV, we tend to classify WR 3 as a single star. Below we provide more facts which strengthen this conclusion.

Indeed, WR 3 was found to be an ordinary X-ray source, i.e. barely detectable in the *ROSAT* All-Sky Survey, $L_{\rm X} = (1.07 \pm 0.76) \times 10^{32}$ erg s^{-1} (Pollock, Haberl & Corcoran 1995), contrary to the expectations of an increased X-ray flux in a potential WR+O colliding-wind binary with a mid- to long-period orbit. Hypothesizing that WR 3 could nevertheless be a WR+c system (WR star and a compact companion, either a neutron star or a black hole), we searched for the presence of rapid periodic flux variations. In an adequately sampled range of frequencies, $f = 0.01$–50 Hz, we found no periodic signals exceeding the 0.007-mag detection limit (Marchenko et al. 1994). Adding to the negative results of the search for rapid variations, we failed to find any variability in the long-term *Hipparcos* photometry (Marchenko et al. 1998b). This was anticipated, considering the relative faintness of WR 3 and the expected low activity of the star. Indeed, more accurate observations (Lamontagne & Moffat 1987) placed WR 3 among the Galactic WN stars with the lowest levels of intrinsic variability, $\sigma_{\rm net} = 0.005$ mag, with $\sigma_{\rm net}$ representing the rms scatter after correction for instrumental effects. Our 1993 photometry gives $\sigma_{\rm net} = 0.007$ mag, the same as in the 1996 data. Both photometric sets give negative results while searched for periodic variability. Hence, we may conclude that the photometric activity of WR 3 does not depend on the epoch of observations and remains at a consistently low level. Practically all known short-period ($P < 30$ d) WR+O binaries show V-shaped dips in their light curves at WR inferior conjunction (Lamontagne et al. 1996). Placing a ∼0.01-mag upper limit on any periodic variations, we conclude that (i) either the hypothetical short-period ($P \lesssim 10$ d) binary has a very low orbital inclination, $i \lesssim 30^\circ$, or (ii) we are dealing with a long-period ($P \gtrsim 10^2$ d) binary. Both cases conform with the non-detection of RV variability.

There are two estimates of the distance to WR 3. One, kinematic based on the Galactic rotation curve, comes from Arnal & Roger (1997): 4.3 ± 0.9 kpc. The second, $d \sim 5.9$ kpc (van der Hucht 2001), is based on spectral types (to yield the absolute magnitudes) and the assumption that WR 3 is a binary system. As the kinematic distance is not based on any assumptions about binarity, we use it and, accounting for the uncertainty in the values of visual extinction, estimate the absolute magnitude of WR 3 to fall in the range $M_V = -2.6$ to -4.6 mag. Taking M_V (WR) ~ -3.2 or M_V (WR) $= -3.7$ – the former is for an average WN3 star (van der Hucht 2001), the latter is the value preferred in modelling (see below) – the first limit leaves no room for an O4 companion. The second limit, $M_V = -4.6$ mag, seems to be slightly more accommodating, however rather extreme as well. Assuming that the hypothetical companion of WR 3 is an O-type bright giant or supergiant, we end up with a systemic M_V far exceeding the -4.6-mag limit. Even an O3−5 dwarf has $M_V = -5.4$ to -5.1 according to Crowther & Dessart (1998), i.e. going over the limit imposed by the kinematic distance to WR 3.

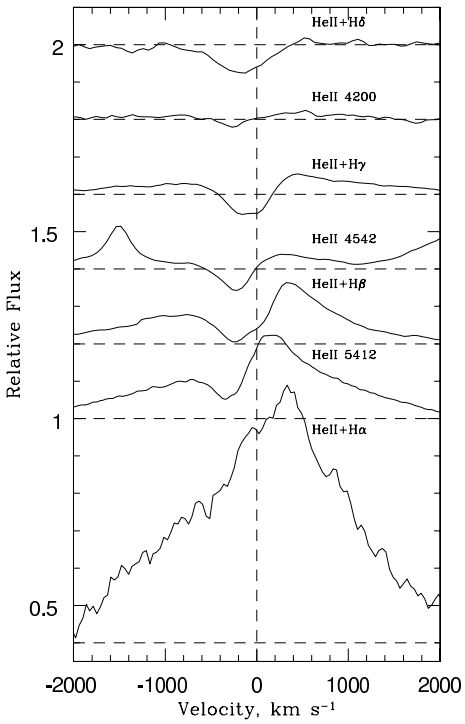

Figure 2. The absorption spectrum of WR 3. The vertical dashed line denotes zero velocities for the He II transitions. Horizontal dashed lines show the assumed levels of the local continuum.

Apparently, we cannot completely rule out the possibility that we are observing a binary with either a long orbital period or with a low orbital inclination. However, the morphology of the well-developed absorption lines looks rather unusual for an ordinary O star (Fig. 2). These lines show a very high blueshift, reaching up to 400 km s^{-1} for some lines, even more extreme than observed in the photospheric lines of some bright Of supergiants (e.g. Crowther & Bohannan 1997). Note the gradual growth of the blueshift in the lines with progressively lower Balmer/Pickering numbers. This is unexpected in the assumed O4 companion, with no sign of its own emission lines. Although at high temperatures the He II lines behave more like H lines (Herrero 2003), in the spectra of hot massive O stars there are no discernible blueshifted He II components (Herrero et al. 1999; Herrero, Puls & Naharro 2002). Hence, we have no doubts that the blueshifted He II absorptions originate in the WR wind. Otherwise, if they belong to an orbiting O star, then given the large shift, these lines should follow a fairly short-period orbit and become redshifted after several days. This is clearly not seen. There are also H components at $v \sim 0$ (Fig. 2; He II + Hγ, He II + Hβ). They may belong to a putative companion. Although we see no signs of systematic orbital motion from the H absorptions, we realize that severe blending with the relatively stronger and, possibly, wider He II absorptions may hide the effect.

In addition, we detect a rapid variability in the P Cygni absorption dips (Fig. 3), which can be related to the formation of those components in the WR wind. The changes barely exceed the detectability thresholds. However, the similarity of variations in different lines provides additional credibility for their reality. We note that P Cygni absorption troughs, if present in the optical spectra of presumably single WR stars, consistently show the highest variability levels

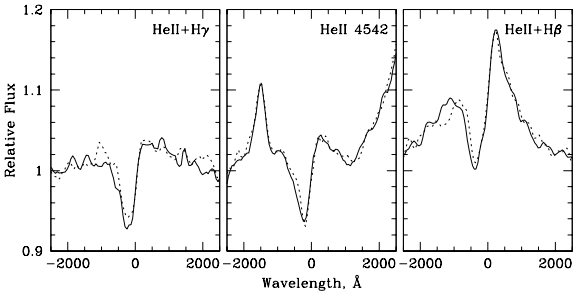

Figure 3. Rapid variability of the absorption components. The full and the dotted lines show the spectra taken at a 30-min interval (OMM data set, 1994).

(cf. Robert 1994; Marchenko et al. 1998a). We do not detect any accompanying variations in the emission parts of the profiles. However, we must admit that this particular data set is not suited for studies of the short-term ($\ll$1 h) variability of the emission profiles in the form of rapidly migrating, narrow emission peaks (e.g. Chené 2003).

There is a noticeable enhancement of the He II + H I absorption dips compared to the He II features in WR 3 (Fig. 2). Assuming that WR 3 is a single star, this clearly points to the presence of hydrogen in the atmosphere of the evolved WNE star. Also note the double-component appearance of some He II + H I absorption profiles, e.g. He II + Hβ. Typically, similar profiles in hot O stars do not show such structuring.

The last plausible possibility to explain the absorption lines as arising in a distinct O star is that we are dealing with a low-probability line-of-sight projection. Confronting this assumption, we again mention the unusual appearance of the absorption spectrum and add that, based on the *Hipparcos* data,[2] WR 3 has no detectable (i.e. separated by $\gtrsim$0.1 arcsec) bright companions. Considering the strength of the WR emission lines and absolute magnitudes of WN3 and O4 stars, the hypothetical companion could be up to six times brighter than the WR star (Smith et al. 1996), thus potentially posing no problems in its detection at this angular separation. What if the companion is much fainter? We use our RCT images and enhance their spatial resolution by choosing an appropriate point-like source in the field and de-convolving the images with a maximum entropy algorithm. This allows us to conclude the following. (i) If there is a visual companion of brightness comparable (within a factor of 2) to that of WR 3, then it should be closer than $\sim$0.4 arcsec, quite in line with the *Hipparcos* data. (ii) If the putative visual companion is much fainter (by a factor of 5), then it must be closer than $\sim$0.7 arcsec. We deem as extremely unlikely a line-of-sight alignment of WR 3 with a massive, early-type star with a separation not exceeding 0.1–0.7 arcsec.

5 MODELLING THE SPECTRUM OF WR 3

To date, the majority of spectroscopic analyses of WN stars have been carried out using non-local thermodynamic equilibrium (NLTE) models that did not account for metal line blanketing or clumping (e.g. Crowther et al. 1995; Hamann, Koesterke & Wessolowski 1995). In only a few cases have clumped, metal line blanketed models been applied to individual stars (e.g. Herald, Hillier & Schulte-Ladbeck 2001). It is widely recognized that such effects need to be taken into account in order to more reliably determine the fundamental parameters of WR stars (Crowther 2003).

5.1 Observational data set

We utilize mean spectroscopy from the present study for the optical regime, revealing spectral features from He II (+ H I), plus numerous N V lines including λ4945, λ4603–20 and O VI λ5290. WR 3 is reminiscent of the WN3 stars WR 46 = HD 104994 and WR 152 = HD 211582 (Crowther et al. 1995). These data sets are supplemented by low-resolution (LORES), short wavelength (SWP) ultraviolet (UV) spectroscopy obtained from the *International Ultraviolet Explorer* (*IUE*) Newly Extracted Spectra (INES) archive, plus near-infrared (near-IR) spectroscopy previously published by Crowther & Smith (1996). The latter indicated the genuine absence of He I λ10830, such that we are unable to obtain stellar parameters from the conventional He I–II ionization balance, in contrast with some other weak-lined WN3 stars (WR 152; Crowther et al. 1995). Instead, we rely solely on the nitrogen ionization balance, N IV–V, for which the only available N IV line is λ1718 in the *IUE* range.

5.2 Technique

We have modelled the UV, optical and near-IR spectrum of WR 3 using CMFGEN (Hillier & Miller 1998), which solves the transfer equation in the comoving frame subject to statistical and radiative equilibrium, assuming an expanding, spherically-symmetric, homogeneous and static atmosphere, allowing for line blanketing and clumping. The stellar radius (R_*) is defined as the inner boundary of the model atmosphere and is located at a Rosseland optical depth of $\sim$20 with the stellar temperature (T_*) defined by the usual Stefan–Boltzmann relation. The atmospheric grid extends from $\sim R_*$ (slightly below) to 100 R_*. There are typically 40 depth points. In the wind these are spaced equally in log(density). In the photosphere they are spaced in log(tau) – approximately half above the connection point between the photosphere and the wind ($\sim$10 km s^{-1} for the WR 3 model, corresponding to $\tau = 0.05$), with half below.

CMFGEN does not solve the momentum equation, so that a density or velocity structure is required. For the supersonic part, the velocity is parametrized with a classical β-type law (with $\beta = 1$), which is connected to a hydrostatic density structure at depth, such that the velocity and velocity gradient match at the interface. This particular value of β provides the best fits to the emission profiles. Moreover, analysis of systematic motions in the wind of WR 3 (small-scale emission details interpreted as out-moving blobs; Chené 2003) provides $\beta R_* = 2.8$–3.2, i.e. $\beta \sim 1$ for $R_* \sim 3$. The subsonic velocity structure is set by the corresponding line-blanketed TLUSTY (v.200) model with $\log g = 4.5$ (Lanz & Hubeny 2003).

One typically obtains wind velocities in WR stars from the UV C IV λ1550 P Cygni profile. However, this line is weak in WR 3 and N V λ1240 is blended with Lyα. Consequently, we obtain a wind velocity from our spectroscopic fit to the strong emission lines of He II λ4686: $v_\infty = 2750 \pm 100$ km s^{-1}, in line with $v_\infty = 2395$ from Niedzielski & Skórzyński (2002), considering the typical $\sim$300 km s^{-1} uncertainty of the latter.

We have assumed a depth-independent Doppler profile for all lines when solving for the atmospheric structure in the comoving frame. In the final calculation of the emergent spectrum in the observer's frame, we have adopted a uniform turbulence of 50 km s^{-1}. Incoherent electron scattering and Stark broadening for hydrogen and helium lines are adopted. We convolve our synthetic spectrum

[2] http://astro.estec.esa.nl/Hipparcos/HIPcatalogueSearch.html.

with a rotational broadening profile, for which we adopt $v \sin i = 200$ km s^{-1}. This value was adopted in order to match the narrow emission lines (e.g. N V).

The atom model contains H I, He I–II, C IV, N IV–V, O IV–VI, Si IV and Fe IV–VIII. In total, 302 super levels, 870 full levels and 7992 NLTE transitions are considered simultaneously. The H/He ratio and CNO elemental abundances are allowed to vary, whilst heavier elements are fixed at solar values (Grevesse & Sauval 1998).

Our approach broadly follows previous studies (e.g. Crowther et al. 1995), such that diagnostic wind lines of nitrogen are selected, namely N IV λ1718 and N V λ4603–20 to derive the stellar temperature, with the mass-loss rate derived from the emission strength of He II λ4686. The luminosity follows from the adopted absolute magnitude. We derive $M_v = -3.7 \pm 0.5$ mag via the kinematical distance of 4.3 ± 0.9 kpc from Arnal & Roger (1997), *ubvr* photometry from Massey (1984) and $E(b–v) = 0.33$ (Hamann & Koesterke 1998), the latter in good agreement with the average $E(b–v) = 0.26 \pm 0.09$ from van der Hucht (2001). If the distance is correct, we have little option but to conclude that WR 3 does not have a massive companion.

The mass-loss rate is actually derived as the ratio $\dot{M}/\sqrt{f}$, where f is the volume filling factor. Generally this may be constrained by fits to the electron scattering wings of the helium line profiles (following Hillier 1991), however such wings are intrinsically weak for WR 3, such that we have adopted a volume filling factor of $f \sim 0.1$, typical for WN stars (Herald et al. 2001).

5.3 Results

As in previous studies of weak-lined WNE stars (Crowther et al. 1995), we derive a high stellar temperature and low wind density for WR 3. The simultaneous presence of N IV λ1718 plus N V λ4603–20 emission allows us to tightly constrain the stellar temperature to $T_* \sim 77$ kK. Temperatures as little as ±2.5 kK different from this predict significantly poorer spectral fits to these lines. The corresponding stellar radius is $R = 3.6$ R$_\odot$, such that the derived luminosity is $L = 4 \times 10^5$ L$_\odot$ with a (clumped) mass-loss rate of $\log \dot{M} = -5.6$. Consequently, the well-known wind momentum ratio does not exceed the single scattering limit for WR 3, with $\dot{M} v_\infty/(L/c) \sim 0.8$. Neglecting clumping we would obtain a mass-loss rate a factor of $1/\sqrt{f}$ higher, i.e. $\log \dot{M} = -5.1$. The spectroscopic comparison between fluxed and rectified spectroscopy and our synthetic spectrum is presented in Fig. 4.

Given the high stellar temperature and low wind density of WR 3, it is one of the few WR stars predicted to show a hard ionizing flux at energies above the He II Lyman edge. The number of ionizing photons shortward of the λ912, λ504 and λ228 edges are $\log N = 49.5$, 49.2 and 47.2 photon s^{-1}, respectively.

We favour the presence of hydrogen in the atmosphere of WR 3, with H/He ∼ 1 by number, based on the model fits of the He II λ10124 (5–4), λ6560 (6–4) + Hα and λ5411 (7–4) profiles, i.e. the lines with a total dominance of the emission component. Overall, we tried to maximize the quality of the fits in the emission parts of the profiles. It has to be admitted that the higher Balmer–Pickering series fail to reproduce shapes of the absorption components, which are uniformly too strong and narrow compared to observations. We have carried out a number of tests, but were unable to reproduce the strong wind emission lines and weak absorption lines simultaneously. We note that the profiles of the strong wind lines formed at several stellar radii are well matched by the adopted velocity law, whilst the problem lies with weak lines formed at depth, just above the hydrostatic core.

With regard to metal abundances, we estimate N/He = 0.003 by number from the N V λ4945 (7–6) recombination line. This is supported by other high lying N V lines λ4520 (9–7), λ11933 (12–10). Carbon and oxygen abundances are less straightforward due to the limited number of suitable diagnostics. Consequently, we adopt C/N = O/N = 0.01 by number, and note that the predicted O V λ1371 is too strong, whilst O VI λ5290 is too weak, suggesting a higher temperature would be required to match the oxygen ionization balance.

For comparison with our results (Table 4), unblanketed NLTE model analyses of WR 3 have previously been carried out by Hamann & Koesterke (1998), also based on the nitrogen line spectrum. They obtained an effective temperature of $T_* = 89$ kK, $\log (L/\mathrm{L}_\odot) = 5.6$, $v_\infty = 2500$ km s^{-1} and an unclumped $\log \dot{M} = -5.1$ with a zero hydrogen content, for an assumed absolute magnitude of $M_V = -3.1$ mag. However, it is unclear whether their higher stellar temperature was derived with the UV N IV λ1718 constraint. We admit that a zero hydrogen content cannot be excluded solely from the relative He II λ5411 – Hβ profiles, but we favour a non-zero value for the diagnostics discussed above, for which inadequacies in absorption components do not play a role. Hydrogen aside, the present result is in rather good agreement with the previous study, suggesting that for WR stars with unusually weak winds, blanketing plays a far less critical role in the revision of stellar properties.

6 TRIANGULAR PROFILES OF WR 3: A CLUE TO SINGLE NATURE?

Because all He II lines and He II/H I blends of WR 3 have relatively weak, triangular profiles (as well as some other WN3 stars, both Galactic as well as LMC/SMC), it seems reasonable to assume they are optically thin. In this case, one can decompose the observed profiles in a simple way – by a series of concentric rings, as was done by Lépine & Moffat (1999) and Ignace et al. (1998) – and derive the emissivity as a function of outward velocity in the wind (Chené 2003). Using a $\beta = 1$ law, the zone of formation of He II 4686 turns out to be quite thin and close to the WR star. Indeed, relying on the parameters from Table 4, we find a peak of the He I 4686 emissivity (Sobolev optical depth unity) at $\sim 2\,R_*$; 65 per cent of the line forming at $r < 2\,R_*$, 90 per cent within $10\,R_*$. In general, the line can be treated as optically thin, except in the innermost regions of the wind ($r < 1.5\,R_*$).

Also, Chené (2003) traced some moving additional emission components on the broad underlying WR profiles, finding extremely high accelerations (they cross the line in about 3 h; cf. in excess of 10 h for other WR stars), compatible with their formation in the strongly accelerating inner part of the wind. This is also in line with the mass-loss rates being relatively small.

WR 152, also WN3, does not show the same high acceleration at all. Its lines are triangular, but not as concave as those of WR 3. Does the triangularity of the profiles have to do more with the wind density than with some specific velocity law? If the density is more important, then one should see some triangular-like profiles in O stars with well-developed optical emission lines. Inspecting our small collection of Hα profiles from late-type O and early-type B supergiants (Morel et al. 2004), we notice that, indeed, once there is a well-developed emission (i.e. EW(em) > EW(abs)), then, invariably, the profile is sharp-pointed and triangular; HD 13854, HD 14134, HD 14818, HD 30614 (probably the best example), HD 37128, HD 41117 and HD 52382 all show this effect. A quick look at the near-IR O spectra from Lenorzer et al. (2002) gives the same impression. However, all lines look triangular in the near-IR *H–K* band regions

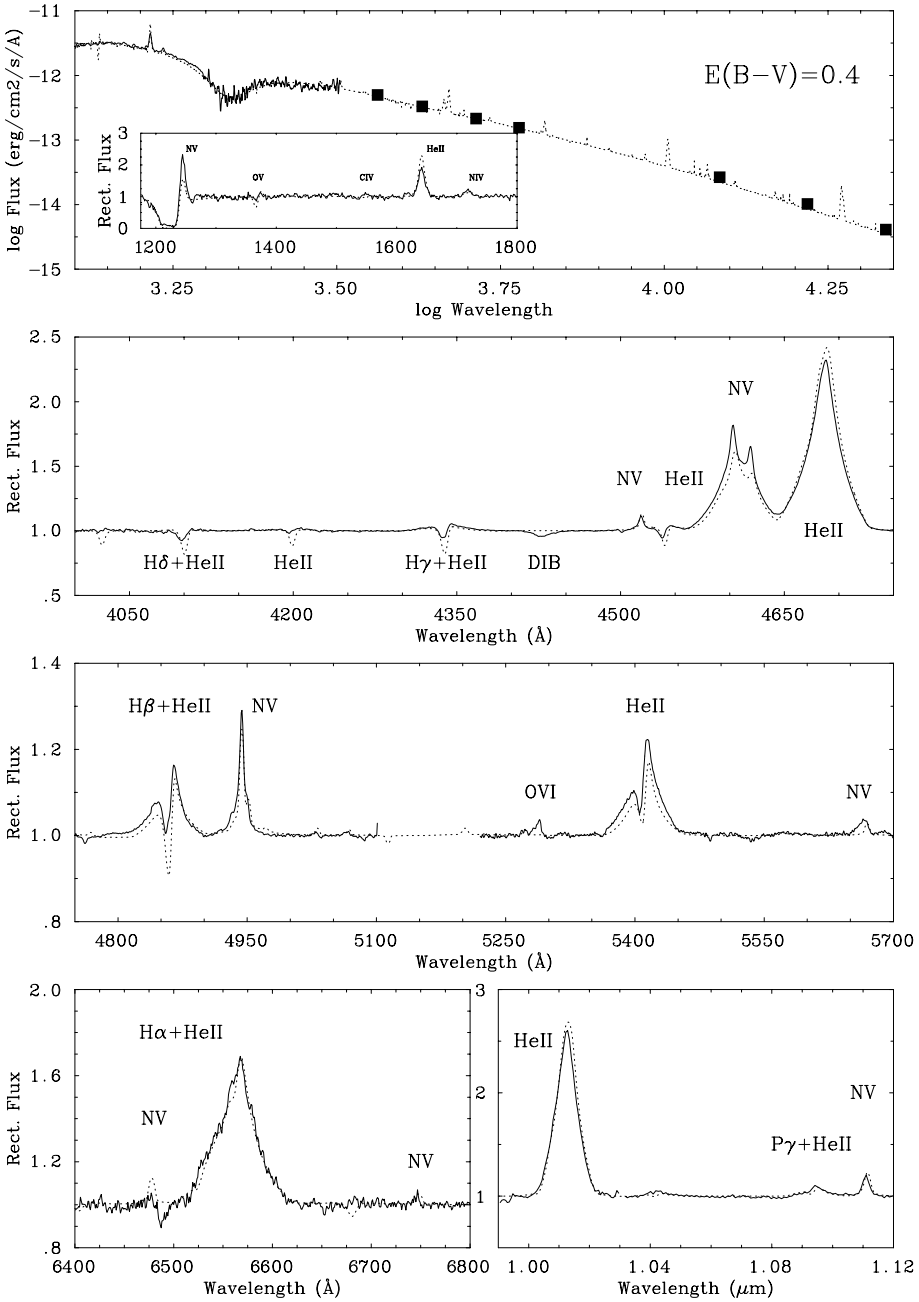

Figure 4. Top panel: spectroscopic comparison between *IUE* spectrophotometry, *ubvr* photometry (Massey 1984) and 2MASS *JHK* photometry for WR 3 and synthetic spectrum (dotted) reddened by $E(B–V) = 0.4$ mag. The inset shows the rectified *IUE* spectrum, together with the synthetic spectrum (dotted), degraded to the resolution of SWP/LORES and includes the correction for atomic Lyα with $\log N(\mathrm{H\,I}) = 21.5$ cm^{-2}. Other panels compare the rectified optical and near-IR observations with our synthetic model (dotted).

if one considers 'stars in transition': WNL–Of–WN/Of–Be–B[e] (Morris et al. 1996). To investigate this point, we obtain a set of models with a variable mass-loss rate. The rest of the parameters are kept constant (as in Table 4). Predictably (Fig. 5), the shape, as well as the strength, of the profiles changes with increased $\dot{M}$. Again, we conclude that one does not need a luminous companion to explain the low intensity of the emission-line profiles in WR 3.

If WR 3 is indeed a single WN3 star, then the presence of relatively strong absorption lines in the optical spectrum points to relatively high hydrogen content. This leads us to classify WR 3 as WN3ha in the system of Smith et al. (1996) or, more generally, as an eWNL star, i.e. a WN star showing hydrogen at its surface (Foellmi et al. 2003b). This may seem unusual for an extremely early-subtype WN star; however, Foellmi et al. (2003a,b) demonstrate that the vast majority of the SMC and many LMC WNE stars exhibit very similar spectra compared to that of WR 3. In the case of the SMC and even the LMC, this is believed to be due to Z-dependent evolution in the pre-WR stage, i.e. as an O star. At low Z, mass loss in the O star is significantly lower and thus less angular momentum is lost from the star (which could have a relatively strong polar wind, all the same). When the WR stage is reached, more mixing occurs and thus more H remains in the WR wind, driven mainly by rotation (Maeder &

Table 4. Model parameters for WR 3.

$R_*(T_*)$ [$R_\odot$ (kK)]	3.6 (77)
$R_{2/3}(T_{2/3})$ [$R_\odot$ (kK)]	3.8 (75)
$\log L/L_\odot$	5.4
$\dot{M}$ ($M_\odot$ yr^{-1})	2.4 10^{-6}
f	0.1
$v_{\rm inf}$ (km s^{-1})	2750
M_V (mag)	−3.7
$X_{\rm H}$ (mass fraction)	20 per cent
$X_{\rm He}$ (mass fraction)	79 per cent
$X_{\rm N}$ (mass fraction)	0.75 per cent

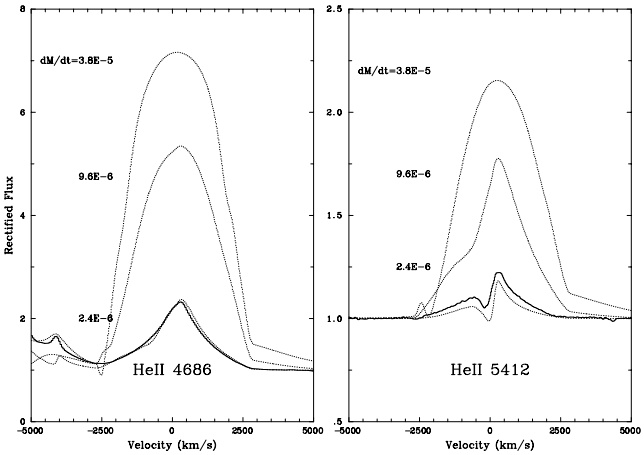

Figure 5. Line profile shapes as a function of mass-loss rate: thin lines, the model profiles; thick lines, the observations.

Meynet 2001). Perhaps WR 3 is an anomalously rapidly rotating WNE star? Or was it a fairly fast rotating object? This may not be implausible, given WR 3's position in the Galaxy towards the anti-centre ($l = 129.18$; van der Hucht 2001), so that its initial metallicity could have been subsolar, using Galactocentric-dependent metallicity observations (e.g. Turbide & Moffat 1993). However, one should note that evolution of the angular momentum strongly depends on the initial mass (Meynet & Maeder 2003), which is not known for WR 3. Hence, all the suggestions about the fast-rotating WR star or, alternatively, fast-rotating WR progenitor must be confirmed observationally. Nevertheless, even modest rotation may explain the appearance of hydrogen in the envelope of a seemingly evolved WN star (Meynet & Maeder 2003). This mechanism may be at work in the case of other Galactic early-type WN stars with a clear presence of hydrogen in their atmospheres, WR 128 (WN4) and WR 152 (Crowther et al. 1995; Nugis & Niedzielski 1995). Similarity between WR 3, WR 128 and WR 152 is even more striking considering their triangular-shaped profiles. Noteworthy, not every weak-lined, early-type WN star with triangular emission profiles shows signs of hydrogen: the short-period binary WR 46 defies this trend (Crowther et al. 1995; Marchenko et al. 2000). The unusually high oxygen content may indicate that WR 46 has passed the eWNL stage. Or, alternatively, the extreme closeness of the companion affects the mass-loss/mixing processes.

7 CONCLUSIONS

Based on the results of spectral analysis, we conclude that WR 3 is a presumably single Galactic WNE star with relatively high H abundance, like many MC WNE stars. This is probably a result of its low initial metallicity, leading to low loss of mass and angular momentum in the O-star progenitor stage. This in turn may lead to an early WN stage in which hydrogen from the upper layers and N and He from the lower layers (where CNO processed material resides) are efficiently mixed by enhanced meridional circulation, so that these elements appear simultaneously in the wind. Rotation is truly a new paradigm that apparently must be taken into account, in this case coupled to the initial metallicity.

ACKNOWLEDGMENTS

AFJM is grateful for financial aid from the Natural Sciences and Engineering Research Council of Canada (NSERC) and Fonds québécois de la recherche sur la nature et les technologies (FQRNT; Quebec). PAC acknowledges financial support from the Royal Society. This study is based in part on INES data from the *IUE* satellite, and *JHK* photometry obtained from the Two-Micron All-Sky Survey (2MASS) at the Infrared Processing and Analysis Center (IPAC). Thanks to John Hillier for providing his stellar atmosphere code CMFGEN. We are also grateful to Jean-Francois Bertrand (former Université de Montréal student) for allowing us to use his collection of spectra of WR 3, and to Adrian Loeff (Senior Software Engineer, EOS Technologies, Inc.) for his help in acquiring the RCT data set. We thank Cédric Foellmi for useful comments. IRAF is distributed by the National Optical Astronomy Observatories, operated by the Association of Universities for Research in Astronomy, Inc., under cooperative agreement with the National Science Foundation.

REFERENCES

Arnal M. E., Roger R. S., 1997, MNRAS, 285, 253
Chené A.-N., 2003, MSc Thesis, Univ. de Montréal
Conti P. S., Leep E. M., Perry D. N., 1983, ApJ, 268, 228
Crowther P. A., 2003, in van der Hucht K. A., Herrero A. and Esteban C., eds, Proc IAU Symp. 212, A Massive Star Odyssey, from Main Sequence to Supernova. Astron. Soc. Pac., San Francisco, p. 47
Crowther P. A., Bohannan B., 1997, A&A, 317, 532
Crowther P. A., Dessart L., 1998, MNRAS, 296, 622
Crowther P. A., Smith L. J., 1996, A&A, 305, 541
Crowther P. A., Smith L. J., Hillier D. J., 1995, A&A, 302, 457
Foellmi C., 2004, A&A, 416, 291
Foellmi C., Moffat A. F. J., Guerrero M. A., 2003a, MNRAS, 338, 360
Foellmi C., Moffat A. F. J., Guerrero M. A., 2003b, MNRAS, 338, 1025
Grevesse N., Sauval A. J., 1998, Space Sci. Rev., 85, 161
Hamann W.-R., Koesterke L., 1998, A&A, 333, 251
Hamann W.-R., Koesterke L., Wessolowski U., 1995, A&A, 299, 151
Herald J., Hillier D. J., Schulte-Ladbeck R. E., 2001, ApJ, 548, 932
Herrero A., 2003, in van der Hucht K. A., Herrero A. and Esteban C., eds, Proc IAU Symp. 212, A Massive Star Odyssey, from Main Sequence to Supernova. Astron. Soc. Pac., San Francisco, p. 3
Herrero A., Corral L. J., Willamariz M. R., Martin E. L., 1999, A&A, 348, 542
Herrero A., Puls J., Naharro F., 2002, A&A, 396, 949
Hillier D. J., 1991, A&A, 247, 455
Hillier D. J., Miller D. L., 1998, ApJ, 496, 407
Ignace R., Brown J. C., Milne J. E., Cassinelli J. P., 1998, A&A, 337, 223
Lamontagne R., Moffat A. F. J., 1987, AJ, 94, 1008
Lamontagne R., Moffat A. F. J., Drissen L., Robert C., Matthews J. M., 1996, AJ, 112, 2227
Lanz T., Hubeny T., 2003, ApJS, 146, 417
Lenorzer A., Vandenbussche B., Morris P., de Koter A., Geballe T. R., Waters L. B. F. M., Hony S., Kaper L., 2002, A&A, 384, 473
Lépine S., Moffat A. F. J., 1999, ApJ, 514, 909

Maeder A., Meynet G., 2001, A&A, 373, 555
Marchenko S. V., Antokhin I. I., Bertrand J.-F., Lamontagne R., Moffat A. F. J., Piceno A., Matthews J. M., 1994, AJ, 108, 678
Marchenko S. V., Moffat A. F. J., Eversberg T., Morel T., Hill G. M., Tovmassian G. H., Seggewiss W., 1998a, MNRAS, 294, 642
Marchenko S. V. et al., 1998b, A&A, 331, 1022
Marchenko S. V., Arias J., Barbá R., Balona L., Moffat A. F. J., Niemela V. S., Shara M. M., Sterken C., 2000, AJ, 120, 2101
Massey P., 1984, ApJ, 281, 789
Massey P., Conti P. S., 1981, ApJ, 244, 173
Meynet G., Maeder A., 2003, A&A, 404, 975
Moffat A. F. J., Lamontagne R., Shara M., McAlister H. A., 1986, AJ, 91, 1392
Morel T., Georgiev L. N., Grosdidier Y., St-Louis N., Eversberg T., Hill G. M., 1999, A&A, 349, 457
Morel T., Marchenko S. V., Pati A. K., Kuppuswamy K., Carini M. T., Wood E., Zimmerman R.K., 2004, MNRAS, 351, 552
Morris P. W., Eenens P. R. J., Hanson M. M., Conti P. S., Blum R. D., 1996, ApJ, 470, 597
Niedzielski A., Skórzyński W., 2002, Acta. Astron., 52, 81
Nugis T., Niedzielski A., 1995, A&A, 300, 237
Pollock A. M. T., Haberl F., Corcoran M. F., 1995, in van der Hucht, K. A., Williams, P. W., eds, Proc. IAU Symp. 163, Wolf–Rayet Stars: Binaries, Colliding Winds, Evolution. Dordrecht, Kluwer, p. 512
Robert C., 1994, Ap&SS, 221, 137
Roberts D. H., Lehár J., Dreher J. W., 1987, AJ, 93, 968
Scargle J. D., 1982, ApJ, 263, 835
Smith L. F., Maeder A., 1998, A&A, 334, 845
Smith L. F., Shara M. M., Moffat A. F. J., 1996, MNRAS, 281, 163
Turbide L., Moffat A. F. J., 1993, AJ, 105, 1831
van der Hucht K. A., 2001, New Astron. Rev., 45, 135

This paper has been typeset from a TEX/LATEX file prepared by the author.